



Research Article

Numerical Simulation of Pounded Area in Drip Irrigation Using by the New Model of Coupling of Two-Phase Navier-Stokes and Richards Equations

Yaser Yekani Motlagh^{1*}, Ali AShraf Sadraddini², Amir Hossein Nazemi³ and Hossein Rezaie⁴

^{1,2,3} Faculty of agriculture, Department of Water Engineering, University of Tabriz, Iran

⁴ Faculty of agriculture, Department of Water Engineering, University of Urmia, Iran

*Corresponding author: yaser.yekani@tabrizu.ac.ir

Article History: Received: January 28, 2016 Revised: May 22, 2016 Accepted: June 21, 2016

ABSTRACT

In drip irrigation, different numerical and analytical models such as Hydrus are used for estimation of wetting pattern. In these models, different parameters are considered as inputs which one of these parameters is pounded area. Amount of this parameter could be obtained by experiment or trial and error methods. Therefore, presenting a model that is able to simulate the pounded area in different time steps and is adaptable to the subsurface flow can increase simulation accuracy and reduce the costs of empirical experiments to determine the pounded area in the numerical models in order to specify wetting pattern. In this paper, a new model for coupling surface (Navier-Stokes, VOF) and subsurface flow equations (Richards) is presented. The method can be used for simulation of the both two phase air-water surface and subsurface flows for determining wetting pattern in the soil in surface drip irrigation. In this model, Richards' equation is discretized with finite volume method and coupled with two-phase Navier-Stokes equations based on a new coupling algorithm. To demonstrate the accuracy of the model, simulation results of soil pounded area in four soil textures and in different discharges were compared to the filed experimental results based on three statistical indices including Mean Error (ME), Root Mean Square Error (RMSE) and Model Efficiency. The results showed that the proposed model has high accuracy to estimate the pounded area and wetting pattern on the soil without field experiments and provided complete data about the velocity, pressure and interface of superficial two-phase flow.

Key words: Drip Irrigation, Equations Coupling, Navier Stocks Equations, Richards Equation, Wetting Pattern

INTRODUCTION

A glance over the history of water and irrigation in the world reveals that several methods for land irrigation have been innovated in recent years. Insufficiency of water, inappropriate atmospheric condition, hilliness, unfavorable quality of water, and lack of access to work force are some limiting factors in development of such methods. Drip irrigation is one of the new methods that has rapidly been developed in different countries. Moisture distribution and wetting pattern of soil in drip irrigation depend to several parameters such as hydraulic specifications of the soil, emitter discharge, evapotranspiration and architectural shape of root (Lazarovitch *et al.*, 2009). There are various empirical, analytical, and numerical methods for describing water infiltration phenomenon under a point source that estimate the wetting pattern of the soil from its hydraulic

specifications. Some of the researchers in this regard are (Philip, 1971; Ben-Asher *et al.*, 1978; Levin *et al.*, 1979; Philip, 1978; Ben-Asher, 1986; Lafolie *et al.*, 1989; Angelakis *et al.*, 1993; Al-Qinna and Abu-Awwad, 2001; Thorburn *et al.*, 2003; Elmaloglou and Malamos, 2006; Chen *et al.*, 2006; Lazarovitch *et al.*, 2007; Bhatnagar and Chauhan, 2008; Keyyan and Peters, 2011; Dabral *et al.*, 2012; Zhigang Liu *et al.*, 2015).

Hydrus is a software package for simulating water, heat, and salt movement in two- and three-dimensional variably saturated porous media, presented by Simunek *et al.*, (1999). In this software, Richards' equation is solved numerically for movement of water in unsaturated soil. Several researchers have used this tool to examine the ability of this model in prediction of wetting pattern in surface and subsurface drip irrigation such as (Skaggs *et al.*, 2004; Cook *et al.*, 2006; Provenzano, 2007; Kandelous and Simunek, 2010; Bufon *et al.*, 2012;

Cite This Article as: Motlagh YY, AA Sadraddini, AH Nazemi and H Rezaie, 2016. Numerical simulation of pounded area in drip irrigation using by the new model of coupling of two-phase Navier-Stokes and richards equations. Inter J Agri Biosci, 5(4): 180-187. www.ijagbio.com (©2016 IJAB. All rights reserved)

Boštjan *et al.*, 2014). The results of these studies indicate that the numerical model of Hydrus has an acceptable accuracy in simulating wetting pattern in surface and subsurface drip irrigations in soils with different textures. Different parameters are considered as input to predict wetting pattern by numerical and analytical models. One of these parameters is ponded area formed on the soil. In fact, when water by a constant discharge is poured to one area of soil, a wet area is appeared. This area is expanded over the time and after a certain duration, a circle area with constant diameter is created. When, diameter of wet circle reaches to a fixed limit, water flow is stable in the soil and this area is called ponded area. One of the problems of analytical and numerical models, especially Hydrus is to specify the ponded area created on the soil; therefore, this area is usually obtained with iterative method or a high cost experimental test. Therefore, presenting a model with ability to simulate the ponded area in different time steps and adjustable to subsurface flow condition is an important issue. One solution to this problem is coupling of surface and subsurface flow equations.

So far, some researchers have employed coupling equations for simulating surface and subsurface flows in surface irrigation and hydrology studies. Morita *et al.* (2002) presented a model for coupling two-dimensional surface and three-dimensional subsurface flows in order to simulate the procedure of Saint-Venant and Richards' equations. Panday and Huyakorn (2004) offered a three-dimensional model for the relationship between surface and subsurface flows applicable to rivers, lakes, ponds and canals. They utilized a two-dimensional zero inertia model for simulating surface flow and Richards' three-dimensional equation for simulating subsurface flow. Zerihun *et al.* (2005a, 2005b) presented a numerical model of coupled surface and subsurface flows equations with an ability to couple it with the model of solute transport in soil for applications in basin and border irrigations. Wöhling *et al.* (2007a, 2007b) provided a numerical model coupling surface and subsurface flow equations in furrow irrigation in a way that root water uptake as a sink term was added to Richards' equation for accurate simulation of the soil wetting pattern. Kong *et al.* (2010) presented a new model coupling surface and subsurface flow equations for simulation of flow in coastal areas, providing surface and subsurface flow simulations from Saint-Venant and Dupuit-Forchheimer equations respectively. Kohne *et al.* (2011) offered a model coupling surface and subsurface flows, applicable in ecological and agricultural systems, which utilized one-dimensional kinematic wave model for simulating surface flow and Richards' two-dimensional equation for subsurface flow.

In this paper, numerical model of coupling Navier-Stokes and Richards equations has been proposed to estimate the ponded area and exact estimation of wetting pattern. Noting the fact that the presented models by previous researchers are not able to simulate the surface flow and its relevant ponded area in drip irrigation with the presented model, it is possible to predict more accurately surface and subsurface wetting pattern in different soil textures with diverse emitter discharges needless to field experiments.

MATERIALS AND METHODS

Equations for surface and subsurface flows and the method of coupling equations

Surface flow

Equations for two-phase water-air surface flow are continuity equation (1) and Navier-Stokes equation (2), respectively (Hirt *et al.*, 1990).

$$\nabla \cdot \rho_m \vec{V}_m = 0 \quad (1)$$

$$\frac{\partial \rho_m \vec{V}_m}{\partial t} + \nabla_m \cdot \nabla \vec{V}_m = -\nabla P + \mu_m \nabla^2 \quad (2)$$

In these relations μ_m is the dynamic viscosity, ρ_m density \vec{V}_m flow velocity, and P is two-phase surface flow pressure (water-air). As surface flow involves two phase of water and air, in this study, VOF model is employed for the two-phase simulation. In this method, a variable (α) is introduced as the volumetric fraction of air in each cell. The volumetric fraction of air is the ratio of air volume to total cell volume. Value of the volumetric fraction of air to each cell is achieved from the following equation (3).

$$\frac{\partial \alpha}{\partial t} + \nabla_m \cdot \nabla \alpha = 0 \quad (3)$$

After determining the value of the volumetric fraction of air in each cell, the values of density and viscosity are achieved from (4) and (5) relations.

$$\rho_m = \alpha \rho_a + (1 - \alpha) \rho_l \quad (4)$$

$$\mu_m = \alpha \mu_a + (1 - \alpha) \mu_l \quad (5)$$

So, there is only one of the following states:

$\alpha = 0$ The cell is empty of air and full of water.

$\alpha = 1$ The cell is full of air.

$0 < \alpha < 1$ The cell is a combination of air and water. The free surface is where the value of α is between zero and one. Therefore, variables and characteristics of each cell is related to one phase or its combination to other phases.

Subsurface Water Flow in Unsaturated Porous Media

The governing Equation for subsurface flow in unsaturated porous media is Richards' non-linear equation (Richards, 1931). This equation is resulted from the combination of conservation of mass and Darcy's Law. Generally, the equation is written in the following form.

$$\frac{\partial \theta}{\partial t} = \nabla \cdot [K(h) \cdot \nabla (h+z)] \quad (6)$$

In which θ is the volumetric water content [$L^3 L^{-3}$] as a function of location, h pressure head [L], t time [T] and K unsaturated hydraulic conductivity of soil [$L T^{-1}$] as a function of pressure head. The Mualem-Van Genuchten hydraulic functions (van Genuchten, 1980; Mualem, 1976), as the most widely used functions, were selected in this study.

$$\theta(h) = \theta_r + \frac{\theta_s - \theta_r}{\left(1 + |\alpha h|^n\right)^m} \quad (7)$$

$$K(h) = K_s \cdot S_e^l \left[1 - \left(1 - S_e^{1/m} \right)^m \right]^2 \quad (8)$$

$$m = 1 - \frac{1}{n} S_e = \frac{\theta_s - \theta_r}{\theta_s - \theta_r} \quad (9)$$

Where θ_s and θ_r are saturated and residual water contents, K_s saturated hydraulic conductivity, and n , α , l are shape parameters.

Coupling Surface and Subsurface Flow Equations

As it is aforementioned, Navier-Stokes and Richards' equations are utilized for simulating surface and subsurface flow, respectively. To this end, coupling equations is used in this study. According to the flowchart in Figure 1, first, surface flow equations (Navier-Stokes equations) are solved. Boundary condition for Navier-Stokes equations is satisfied by considering the infiltration rate which obtained using potential gradient on interface of water-soil, resulted from solving Richards' equation in preceding time step. By solving Navier-Stokes equations as two-phase flow model, the interface between air and water is characterized and the velocity and pressure for air and water are determined. Then, the determined water pressures (h) in the nodes of the water-soil interface are used as boundary condition values for solving Richards' equation in the present time step. This staggered process is followed until achieving to the final result. In this paper, the open source CFD package, Open Source Field Operation and Manipulation ('OpenFOAM'), which is based on the work of Weller et al. (1998) was used for the flow simulation. The discretisation of the flow governing equations in the 'OpenFOAM' is based on the finite volume method formulated with the collocated variable arrangement, with the pressure and velocity solved by segregated methods. Open FOAM is a C++ code library of classes for writing CFD codes, which includes a well-tested and validated RANS capability, and the VOF model for the two-phase flow modeling. Several numerical convection differencing schemes are available in OpenFOAM, including upwind, central difference, QUICK and flux limiters schemes. In this study, the numerical code is developed. Firstly, Richards' equations are written in C++ programming with finite volume method. Then, it is coupled with two-phase Navier-Stokes equations and VOF method based on presented algorithm.

Model Accuracy Assessment Criteria

To analyze the simulated values based on the observed data in this study, four statistical criteria of root mean square error (RMSE), coefficient of determination (R^2), model efficiency (EF), and mean error (ME) are utilized. Model efficiency relation is presented by Smith et al. (1996). The maximum value of this parameter is one and the closer the EF value to one, the higher the model efficiency. The relations for calculating root mean square error, coefficient of determination, model efficiency, and mean error are:

$$RMSE = \sqrt{\frac{1}{n} \sum_{i=1}^n (x_i - y_i)^2} \quad (10)$$

$$R^2 = \frac{(\sum_{i=1}^n x_i y_i - \frac{1}{n} \sum_{i=1}^n x_i \sum_{i=1}^n y_i)^2}{(\sum_{i=1}^n x_i^2 - \frac{1}{n} (\sum_{i=1}^n x_i)^2) (\sum_{i=1}^n y_i^2 - \frac{1}{n} (\sum_{i=1}^n y_i)^2)} \quad (11)$$

$$EF = \frac{(\sum_{i=1}^n (x_i - \bar{x})^2 - \sum_{i=1}^n (x_i - y_i)^2)}{\sum_{i=1}^n (x_i - \bar{x})^2} \quad (12)$$

$$ME = \frac{\sum_{i=1}^n (y_i - x_i)}{n} \quad (13)$$

Where X_i and Y_i are the observed and modeled values respectively, \bar{x} is the mean of the observed (measured) data and n is the number of observations.

Characteristics of Simulated Numerical Model

Validity of the numerical model, in this study, is analyzed through field experiment results by Alibabaei et al. (1997). They used four kinds of soils with the shown characteristics in Table 1. Alibabaei et al. (1997) in their field studies measured the ponded area using an emitter with different discharges in different soil textures and periods at 3000 seconds.

Mesh study and Boundary Conditions

In Figure 2, three-dimensional scheme of the simulated flow in this study is presented. This schematic model includes three sectional areas of surface, subsurface flows, and emitter outflow. The solution field is considered a cylinder with 50 centimeters radius and 60 centimeters height in which the height of surface flow section is 2 millimeters (distance of out flowing water from emitter to soil). Dimensions of the emitter are defined as a cylinder with 2 millimeters diameter and 2 centimeters height. As it is clear from Figure 2, the flow domain has a symmetrical geometry to central axis passing from emitter (A-A); therefore, only a sector of the presented domain in Figure 2, is assigned for mesh generation and the problem is solved as a case of axial symmetry. Figure 3, illustrates a section of mesh network near the emitter comprising fields of surface, subsurface and emitter flows. The applied mesh contained structured grids and the number of selected meshes, in this study, is 26500. Moreover, in some part of the mesh network such as near the emitter, for achieving high accuracy the mesh densities are increased.

In this study, according to Figure 3, the location of outflowing water from emitter is considered as the velocity boundary condition at the inlet of system and the velocity is calculated regarding to sectional area of emitter in different discharges. The wall of emitter is considered also as the wall boundary condition and other surface flow boundaries are regarded as boundary condition for atmospheric pressure. Boundary condition of interface flow for surface and subsurface is considered as a boundary condition varying with time and determined from solving the coupled surface and subsurface equations according to the explanations in the previous section. For subsurface flow boundary condition of free drain ($\nabla H = 0$) is considered in lower and side sections.

Numerical solution

In this section, the discretization of equations by the finite volume method is presented according to the considered boundary conditions. The equation (14) indicates the general discretized form of Richards' equation for control volume V_p as depicted in Figure 4.

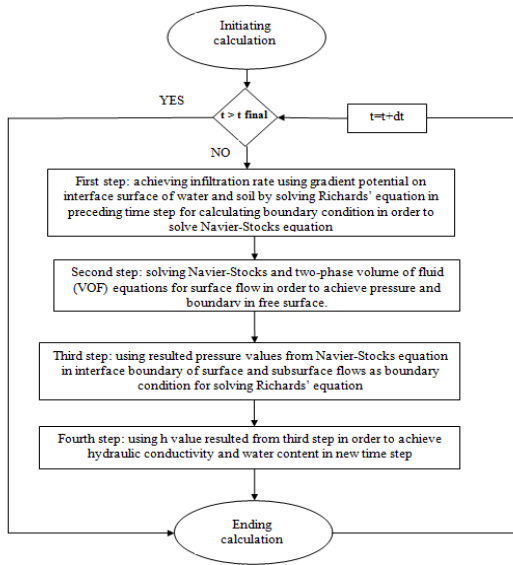


Fig. 1: Flowchart for Coupling Surface and Subsurface Flow Equations

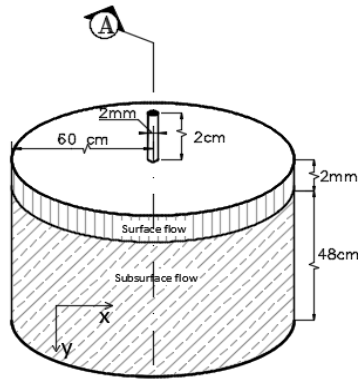


Fig. 2: Scheme of Simulated Three-dimensional Model

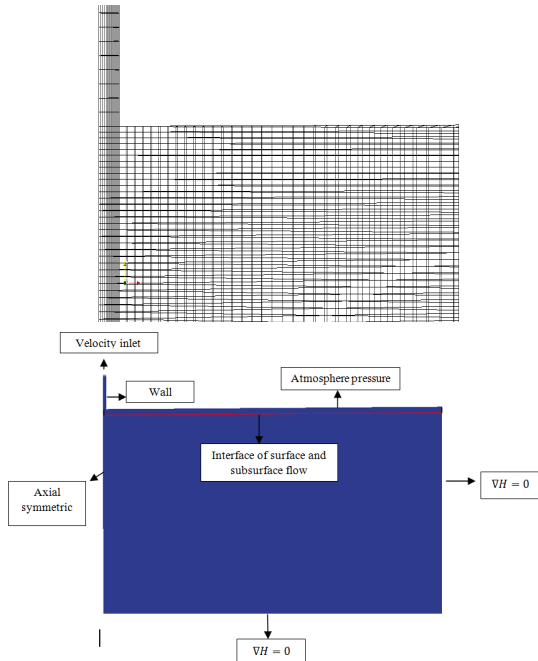


Fig. 3: Mesh and boundary condition configuration.

$$\int_{t_1}^{t_2} \int_V \frac{\partial \theta}{\partial t} dV = \int_{t_1}^{t_2} \int_V \frac{\partial}{\partial x} \left(k_x \frac{\partial h}{\partial x} \right) dV + \int_{t_1}^{t_2} \int_V \frac{\partial}{\partial y} \left(k_y \frac{\partial h}{\partial y} \right) dV + \int_{t_1}^{t_2} \int_V \frac{\partial}{\partial z} \left(k_z \frac{\partial h}{\partial z} \right) dV \quad (14)$$

The general equation after time and space discretization is as following:

$$(\theta_p^{t+\Delta t, m+1} - \theta_p^t) \Delta z = \left(k_x \frac{h_x^{t+\Delta t, m+1} - h_p^{t+\Delta t, m+1}}{\Delta x} - k_w \frac{h_p^{t+\Delta t, m+1} - h_w^{t+\Delta t, m+1}}{\Delta x} \right) + \left(k_n \frac{h_n^{t+\Delta t, m+1} - h_p^{t+\Delta t, m+1}}{\Delta y} + k_n^t - k_s^t \frac{h_p^{t+\Delta t, m+1} - h_s^{t+\Delta t, m+1}}{\Delta y} - k_s^t \right) \quad (15)$$

Where the superscripts n and m denote the time and iteration levels, respectively. A truncated Taylor series for the water content at the new time step and new iteration $\theta^{t+\Delta t, m+1}$ with respect to h has the form:

$$\theta_p^{t+\Delta t, m+1} = \theta_p^{t+\Delta t, m} + \left(\frac{d\theta}{dh} \right)^{t+\Delta t, m} (h_p^{t+\Delta t, m+1} - h_p^{t+\Delta t, m}) \quad (16)$$

By substituting of this equation in equation (15), the general form of the resulted linear equation is:

$$\alpha h_N^{t+\Delta t, m+1} + \beta h_s^{t+\Delta t, m+1} + \gamma h_w^{t+\Delta t, m+1} + p h_E^{t+\Delta t, m+1} + \lambda h_p^{t+\Delta t, m+1} = \varepsilon \quad (17)$$

$$\alpha = k_N^t \frac{\Delta t}{\Delta x^2} \quad \beta = k_s^t \frac{\Delta t}{\Delta x^2} \quad \gamma = k_w^t \frac{\Delta t}{\Delta x^2} = k_s^t \frac{\Delta t}{\Delta x^2} \quad (18)$$

$$\lambda = - \left[(k_n^t + k_s^t + k_w^t + k_s^t) \frac{\Delta t}{\Delta x^2} + C_p^t \right] \quad (19)$$

$$\varepsilon = \theta_p^{t+\Delta t, m} - \theta_p^t - C_p^t h_p^{t+\Delta t, m} + (k_s^t - k_n^t) \left(\frac{\Delta t}{\Delta x^2} \right) \quad (20)$$

For the right side boundary condition, equation (17) is modified as:

$$P=0, \quad \alpha h_N^{t+\Delta t, m+1} + \beta h_s^{t+\Delta t, m+1} + \gamma h_w^{t+\Delta t, m+1} + \lambda h_p^{t+\Delta t, m+1} = \varepsilon \quad (21)$$

$$\lambda = - \left[(k_n^t + k_s^t + k_w^t + k_s^t) \left(\frac{\Delta t}{\Delta x^2} \right) + C_p^t \right] \quad (22)$$

$$\varepsilon = \theta_p^{t+\Delta t, m} - \theta_p^t - C_p^t h_p^{t+\Delta t, m} + (k_s^t - k_n^t) \left(\frac{\Delta t}{\Delta x^2} \right) \quad (23)$$

Also in lower boundary condition, equation (17) can be written as:

$$\beta=0, \quad \alpha h_N^{t+\Delta t, m+1} + \gamma h_w^{t+\Delta t, m+1} + p h_E^{t+\Delta t, m+1} + \lambda h_p^{t+\Delta t, m+1} = \varepsilon \quad (24)$$

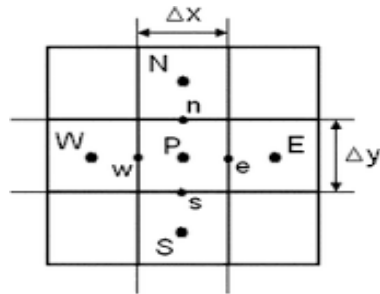
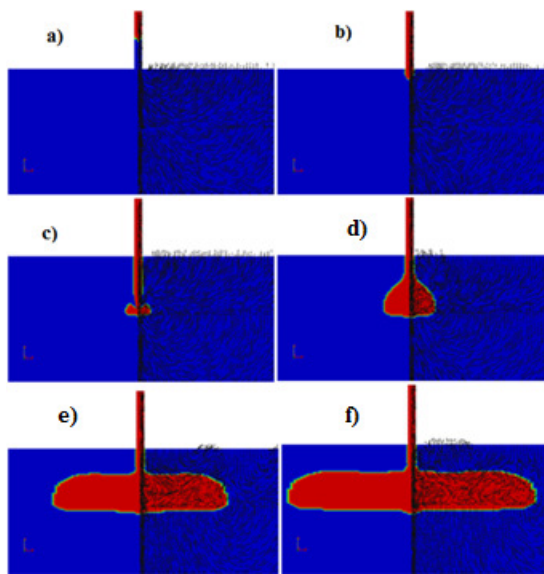
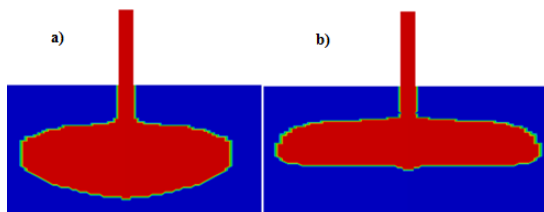
RESULTS AND DISCUSSION

Qualitative Results of Surface and Subsurface Flow Simulation (water content volume fraction contours)

Figure 5, shows the qualitative results of surface and subsurface flow simulations with discharge of 2.62 L/h in a loamy soil. In the presented figures, the red color indicates water and blue indicates the air. Also, in the presented figures, velocity vectors are shown only for half of solution area due to symmetry of flow field. According to figures (5-a) and (5-b), in the initial moments the water drop inside the emitter is coming down. According to

Table 1: Physical Characteristics of Soil

Soil texture	$\theta_s (cm^3 cm^{-3})$	$\theta_r (cm^3 cm^{-3})$	$\alpha (cm^{-1})$	$n (-)$	$k_s (cm hr^{-1})$	I	sand	silt	Clay
Silty clay	0.45	0.0931	0.0124	0.3901	15.12	0.5	16.6	41	42.4
loam	0.43	0.0711	0.0138	1.413	17.75	0.5	39.4	35	25.4
Sandy clay loam	0.044	0.0695	0.0162	1.3757	41.04	0.5	36.6	26	27.41
clay	0.429	0.0991	0.0157	1.3257	8.84	0.5	14	35	51

**Fig. 4:** Discretization with finite Volume**Fig. 5:** Qualitative Results of Surface and Subsurface Flow Simulation with Discharge 2.63 L/h in Soil with loam Texture.**Fig. 6:** Qualitative Results of Surface and Subsurface Flow a: Sandy clay loam soil b: Clay soil

shape of velocity vectors in water and air parts, the air fluid is moving out from the emitter by coming down the water. In figure (5-c), water drop is broken after exiting the emitter and contacting the earth. In figure (5-d), the water flows on the earth without infiltration in the soil after contacting the earth. The velocity vectors in the water section indicate that water flow inside the soil is strongly vortical. According to figure (5-e), in next moments, the water flows on the surface and then infiltrates inside the soil. The level of infiltration flow and

flow discharged into the earth area strongly depends on hydraulic conductivity of soil. As figure (5-f) shows, the pounded area and the water depth inside the soil area will be larger by flowing and infiltrating the water inside the soil. The results show that after a certain time, the radius of pounded area is not changed and just the water infiltrates inside the soil through this area. In fact, this is the same radius which obtained by field experiments and considered as input in the numerical models such as Hydrus. As indicated, the presented model in this study is able to obtain the area directly. In figure (6), the numerical solution results are presented for two kinds of soil including sandy loam and clay textures with different hydraulic features in a certain time and identical discharge (2 L/h). According to the figure, the pounded area of soil with higher hydraulic conductivity (soil with sandy clay loam texture) is smaller than soil with lower hydraulic conductivity (soil with clay texture), but the wetted depth in clay loam soil is more. For more survey, the simulated qualitative results conducted on different textures and discharges of soils are presented in following to confirm the results.

Quantitative results of numerical simulation for wetting pattern advance

The radius of pounded area as a function of time with different discharges and in different textures is compared to the experimental results in figure (7). The results of these figures reveal that the results provided by the model are consistent to the field results. Moreover, these figures show that the radius of pounded area was increased immediately and reached on a fixed value after 10-15 minutes. The radius is increased by decreasing hydraulic conductivity so that heavier soil texture increases the pounded area radius. The figures confirm that the time needed to reach steady state is increased by increasing the discharge of emitter.

Precision Assessment of the presented Model

The radius distance of wetting pattern from to emitter location in different textures and discharges has been compared to the statistical indices to examine the accuracy of the proposed model. The coefficients of R^2 in different textures and discharges of soil in accordance to table (2) which is (0.967-0.998) indicates high ability of this model to simulate the wetting pattern. For more survey, the value of RMSE and EF of model for pounded area index is shown in table (2). Given the results in these tables, the proposed model has low RMSE value. Also, EF in the proposed model is close to one and this indicates high efficiency of the proposed model. In table (3), percent of relative error of predicted value and the proposed model is shown. As shown in table (3), the percent of predicted relative error of pounded area with the proposed model is (0.48- 13.46) and absolute mean of 4.67, so the proposed model has high ability to estimate the wetted area.

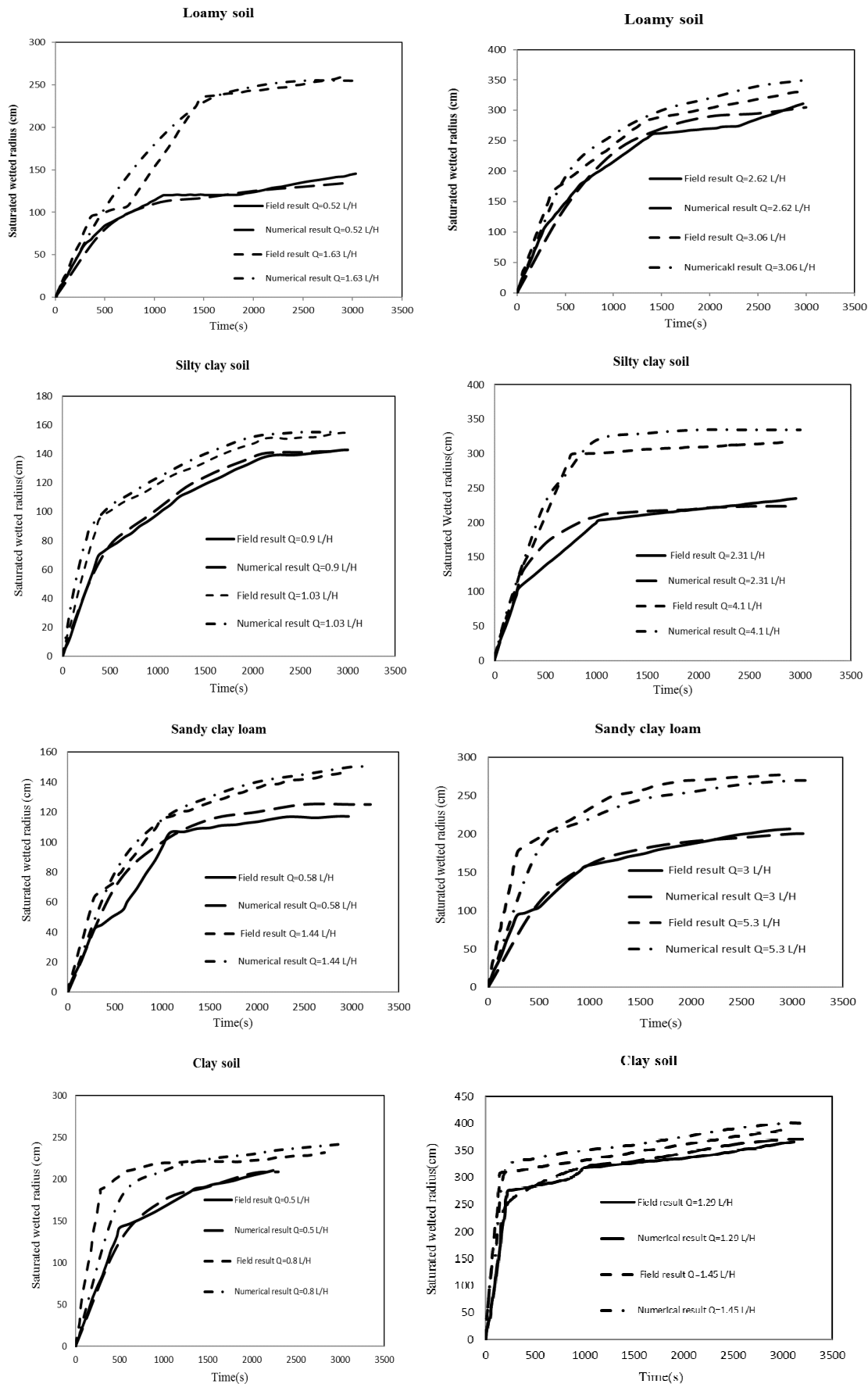


Fig. 7: Results of ponded area in drip irrigation with different soil textures and discharges

Table 2: Mean squared error values, efficiency values and coefficient of determination in different soil textures and discharges between field values and values resulted from presented numerical model

R ²	EF	RMSE	q(lit/hr)	Soil texture
0.998	0.996	2.80	0.52	loam
0.991	0.976	9.27	1.63	loam
0.967	0.991	9.31	2.62	loam
0.971	0.982	14.30	3.06	loam
0.998	0.998	2.10	0.90	Silty clay
0.997	0.996	3.16	1.03	Silty clay
0.984	0.988	8.67	2.30	Silty clay
0.998	0.999	9.49	4.10	Silty clay
0.967	0.959	8.10	0.58	Sandy clay loam
0.992	0.993	3.86	1.44	Sandy clay loam
0.993	0.996	4.03	3.00	Sandy clay loam
0.978	0.985	10.59	5.31	Sandy clay loam
0.987	0.987	7.85	0.50	Clay
0.968	0.997	12.86	0.80	Clay
0.996	0.998	6.47	1.29	Clay
0.972	0.973	21.35	1.45	Clay

Table 3: Percent of relative error for estimated values with presented numerical model and field values

Relative error %	Saturated wetted radius simulation value (mm)	Saturated wetted radius observed value (mm)	T (s)	Q (lit/hr)	Soil texture
4	80	82	500	0.52	Loam
-3.51	110	114	1000	0.52	Loam
0.81	125	124	2000	0.52	Loam
1.48	137	135	3000	0.52	Loam
2.70	190	185	500	3.06	Loam
7.88	260	241	1000	3.06	Loam
3.23	320	310	2000	3.06	Loam
5.74	350	331	3000	3.06	Loam
1.32	77	76	500	0.9	Silty clay
2.88	107	104	1000	0.9	Silty clay
1.45	140	138	2000	0.9	Silty clay
-0.70	141	142	3000	0.9	Silty clay
9.68	170	155	500	2.3	Silty clay
3.47	209	202	1000	2.3	Silty clay
0.91	222	220	2000	2.3	Silty clay
-4.27	224	234	3000	2.3	Silty clay
13.46	59	52	500	0.58	Sandy clay loam
3.09	100	97	1000	0.58	Sandy clay loam
7.14	120	112	2000	0.58	Sandy clay loam
5.93	125	118	3000	0.58	Sandy clay loam
-7.22	180	194	500	5.31	Sandy clay loam
-5.58	220	233	1000	5.31	Sandy clay loam
-5.56	255	270	2000	5.31	Sandy clay loam
-2.88	270	278	3000	5.31	Sandy clay loam
-11.97	125	142	500	0.5	Clay
4.79	175	167	1000	0.5	Clay
1.97	207	203	2000	0.5	Clay
0.48	209	208	2300	0.5	Clay
4.69	335	320	500	1.45	Clay
5.11	350	333	1000	1.45	Clay
3.88	375	361	2000	1.45	Clay
3.72	390	376	2500	1.45	Clay
3.09	400	388	3000	1.45	Clay

Conclusion

In this study, a new model to estimate the soil wetting pattern in surface drip irrigation is presented with coupling the Navier-Stocks and Richards' equations. In simulation of the soil moisture pattern under a water

source, most of the relevant models need estimation of the surface ponded area for using as the upper boundary condition, which is usually determined through a trial and error method or field experiments. This study attempts to develop a model which does not require to estimation of the mentioned upper boundary condition. In this regard, the Open FOAM code, which is an open source CFD code with high abilities, is developed. This code is written based on the finite volume method and in object-oriented C++ programming. In this study, firstly, Richards' equation is discretized through the finite volume method and written in C++ programming. Then, according to the presented algorithm, it is coupled with the two-phase surface equations. Results of the presented model are compared with available experimental data for four soil textures and different discharges which confirms the high ability and accuracy of the model in simulation of wetting pattern with minimum error rate and maximum efficiency. This model also offers complete information about field of velocity, pressure and interface of the two-phase surface and subsurface flows.

REFERENCES

- Alibaba A, 1997. Comparison Two Methods of Dripper and Constant Loading in Measurement of Hydraulic Conductivity and Providing a Comparative Model. Master Thesis of Irrigation and Drainage, Agriculture College, Tabriz University.
- Al-Qinna MI and AM Abu-Awwad, 2001. Wetting Patterns under Trickle Source in Arid Soils with Surface Crust. *J Agric Engin Res*, 80: 301-305.
- Angelakis AN, DE Rolston, TN Kadir and VH Scott, 1993. Soil water distribution under trickle source. *J Irrig Drain Engin-ASCE*, 119: 484-500.
- Ben-Asher J, DO Lomen and AW Warrick, 1978. Linear and nonlinear models of infiltration from a point source. *Soil Sci Soc Amer J*, 42: 3-6.
- Ben-Asher J, 1986. Infiltration and water extraction from trickle irrigation source: the effective hemisphere model. *Soil Sci Soc Amer J*, 50: 882-887.
- Bhatnagar PR and HS Chauhan, 2008. Soil water movement under a single surface trickle source. *Agric Water Manag*, 95: 799-808.
- Bojanala, C Kechavarzi, F Coulon, and M Pintar, 2014. Numerical investigation of the influence of texture, surface drip emitter discharge rate and initial soil moisture condition on wetting pattern size. *Irrig Sci*, 32: 421-436.
- Bufon VB, RJ Lascano and C Bednarz, 2012. Soil water content on drip irrigated cotton: comparison of measured and simulated values obtained with the Hydrus 2-D model. *Irrig Sci*, 30: 259-273.
- Chen JM, YC Tan, and YZ Wu, 2006. A study of the infiltration of trickle irrigation. 7th International Micro Irrigation Congress. September 10-16, Kuala Lumpur, Malaysia.
- Cook, FJ, P Fitch, PJ Thorburn, PB Charlesworth, and KL Bristow, 2006. Modeling trickle irrigation: Comparison of analytical and numerical models for estimation of wetting front position with time. *Environmental Modelling & Software*, 21: 1353-1359.

- Dabral PP, PK Pandey, A Pandey, KP Singh, and M Sanjoy, 2012. Modelling of wetting pattern under trickle source in sandy soil of Nirjuli, Arunachal Pradesh (India). *Irrig Sci*, 30: 287–292.
- Elmaloglou S and N Malamos, 2006. A methodology for determining the surface and vertical components of the wetting front under a surface point source, with root water-uptake and evaporation. *Irrig Drain*, 55: 99–111.
- Hirt CW and BD Nicholas, 1992. Volume of fluid (VOF) method for the dynamics of free boundaries. *J Computer Phys*, 39: 201–225.
- Kandelous MM, and J Simunek, 2010a. Comparison of numerical, analytical, and empirical models to estimate wetting patterns for surface and subsurface drip irrigation. *Irrig Sci*, 28: 435–444.
- Keyyan M, and RT Peters, 2011. Wetting pattern models for drip irrigation: new empirical model. *J Irrig Drain Engin-ASCE*, 137: 530–537.
- Kohne JM, T Wohling, and V Pot, 2011. Coupled simulation of surface runoff and soil water flow using multi-objective parameter estimation. *J Hydrol*, 403: 141–156.
- Kong J, P Xin, Z Song, and L Li, 2010. A new model for coupling surface and subsurface water flows: With an application to a lagoon. *J Hydrol*, 390: 116–120.
- Lafolie F, R Geunneelon, van and MTh Genuchten, 1989b. Analysis of water flow under trickle irrigation: II. Experimental evaluation. *Soil Sci Soc Amer J*, 53: 1318–1323.
- Lazarovitch N, AW Warrick, A Furman, and J Simunek, 2007. Subsurface water distribution from drip irrigation described by moment analyses. *Vadose Zone J*, 6: 116–123.
- Lazarovitch N, M Poulton, A Furman, and AW Warrick, 2009. Water distribution under trickle irrigation predicted using artificial neural networks. *J Eng Math*, 64: 207–218.
- Levin I, PC Van Rooyen, and FC Van Rooyen, 1979. The Effect of Discharge Rate and Intermittent Water Application by Point-source Irrigation on the Soil Moisture Distribution Pattern. *Soil Sci Soc Amer J*, 43: 8–16.
- Morita M and BC Yen, 2002. Modeling of conjunctive two dimensional Surface-three-dimensional subsurface flows. *J Hydraulic Eng*, 128: 184–200.
- Panday S, and PS Huyakorn, 2004. A fully coupled physically based spatially-distributed model for evaluating surface/subsurface flow. *Adv Water Resour*, 27: 361–382.
- Philip JR, 1971. General theorem on steady infiltration from surface source, with application to point and line sources. *Soil Sci Soc Amer J*, 35: 867–871.
- Philip RJ, 1984. Travel time from buried and surface infiltration point sources. *Water Res Res*, 20: 990–994.
- Provenzano G, 2007. Using Hydrus-2D simulation model to evaluate wetted soil volume in subsurface drip irrigation systems. *J Irrig Drain Engin-ASCE*, 133: 342–349.
- Richards L, 1931. Capillary conduction of liquids through porous mediums. *Physics*, 1: 318–333.
- Simunek J, M Sejna, and MTh van Genuchten, 1999. The Hydrus-2D software package for simulating two-dimensional movement of water, heat and multiple solutes in variably saturated media, Version 2.0. Rep. IGCWMC-TPS-53, p 251, International Ground Water Model. Cent, Colo. Sch. of Mines, Golden, CO.
- Shani UR, J Hanks, E Bresler, and CAS Olivira, 1987. Field method for estimating hydraulic conductivity and metric potential water content relations. *Soil Sci Soc Am J*, 51: 298–302.
- Skaggs TH, TJ Trout, J Simunek and PJ Shouse, 2004. Comparison of Hydrus-2D simulations of drip irrigation with experimental observations. *J Irrig Drain Engin-ASCE*, 130: 304–310.
- Smith JU, P Smith and Addiscott, 1996. TM Quantitative methods to evaluate and compare soil organic matter (SOM) models. In: Powlson DS, Smith P, Smith JU (eds) Evaluation of soil organic matter models using existing long-term datasets NATO Advanced Research Workshop: Papers, NATO ASI Series 1 edn, Vol 38, NATO ASI series I global environmental change, vol 38, Springer, Heidelberg.
- Subbaiah R, 2013. A review of models for predicting soil water dynamics during trickle irrigation. *Irrig Sci*, 31: 225–258.
- Thorburn PJ, FJ Cook, and KL Bristow, 2003. Soil-dependent wetting from trickle emitters: Implications for System Design and Management. *Irrig Sci*, 22: 121–127.
- Van Genuchten MTh, 1980. A closed-form equation for predicting the hydraulic conductivity of unsaturated soils. *Soil Sci Soc Amer J*, 44: 892–898.
- Weller HG, G Tabor, H Jasak and CA Fureby, 1998. Tensorial Approach to Computational Continuum Mechanics Using Object-Oriented Techniques. *Computer Phys*, 12: 620–631.
- Wöhling Th, and GH Schmitz, 2007a. Physically based coupled model for simulating 1D surface–2D subsurface flow and plant water uptake in irrigation furrows. I: Model development. *J Irrig Drain Engin-ASCE*, 133: 538–547.
- Wöhling Th, and GH Schmitz. 2007b. Physically based coupled model for simulating 1D surface–2D subsurface flow and plant water uptake in irrigation furrows. II: Model Test and Evaluation. *J Irrig Drain Engin-ASCE*, 133: 548–558.
- Zerihun D, A Furman, A Warrick, and CA Sanchez, 2005a. A coupled surface-subsurface solute transport model for irrigation borders and basins: I. Model development. *J Irrig Drain Engin-ASCE*, 131: 396–406.
- Zerihun D, CA Sanchez, A Furman, and AW Warrick, 2005b. A coupled surface-subsurface solute transport model for irrigation borders and basins, II. Model evaluation. *J Irrig Drain Engin-ASCE*, 131: 407–419.
- Zhigang Liu, P Li, Y Hu, and W Jizhang, 2015. Wetting patterns and water distributions in cultivation media under drip irrigation. *Comput Electr Agric*, 112: 200–208.